Bioorganic & Medicinal Chemistry Letters 30 (2020) 127576

Contents lists available at ScienceDirect

Bioorganic & Medicinal Chemistry Letters

journal homepage: www.elsevier.com/locate/bmcl

Design and synthesis of 4-Aminoquinoline-isoindoline-dione-isoniazid triads as potential anti-mycobacterials

Anu Rani[a], Matt D. Johansen[b], Françoise Roquet-Banères[b], Laurent Kremer[b,c], Paul Awolade[d], Oluwakemi Ebenezer[d], Parvesh Singh[d], Sumanjit[a], Vipan Kumar[a,*]

[a] Department of Chemistry, Guru Nanak Dev University, Amritsar 143005, Punjab, India
[b] Institut de Recherche en Infectiologie (IRIM) de Montpellier, CNRS, UMR 9004 Université de Montpellier, France
[c] INSERM, IRIM, 34293 Montpellier, France
[d] School of Chemistry and Physics, University of KwaZulu-Natal, P/Bag X54001, Westville, Durban, South Africa

ARTICLE INFO

Keywords:
4-aminoquinoline-isoindoline-dione-isoniazid
Anti-mycobacterial activity
Cytotoxicity
Selectivity index
Molecular docking

ABSTRACT

A series of 4-aminoquinoline-isoindoline-dione-isoniazid triads were synthesized and assessed for their anti-mycobacterial activities and cytotoxicity. Most of the synthesized compounds exhibited promising activities against the mc^{2}6230 strain of *M. tuberculosis* with MIC in the range of 5.1–11.9 μM and were non-cytotoxic against Vero cells. The conjugates lacking either isoniazid or quinoline core in their structural framework failed to inhibit the growth of *M. tuberculosis*; thus, further strengthening the proposed design of triads in the present study.

Tuberculosis (TB), an infectious disease caused by the bacterium, *Mycobacterium tuberculosis*, has resulted in chronic granulomatous lesions in the lungs, which can be accompanied by extra-pulmonary infection foci in the skin, brain and lymph nodes[1]. The disease is the major cause of death after the Human Immune-deficiency Virus (HIV), accounting for 1945 deaths every day[2]. World Health Organization (WHO) estimated that at least 10 million people developed TB with 1.3 million deaths in 2017[3]. Despite the availability of an important variety of drugs, TB remains a significant global health threat[4–5]. The foremost obstacle in the total eradication of TB is the development of resistance of *M. tuberculosis* to many existing drugs, which has led to the appearance of multidrug-resistance (MDR) and extensively drug-resistant (XDR) strains[6–11]. Also, TB and HIV co-infection is a major concern with nearly two-thirds of the patients diagnosed with TB also being HIV-1 seropositive[12]. The re-designing and re-positioning of known anti-TB scaffolds is an effective strategy for the development of new frameworks with favorable pharmacological profiles such as high efficacy and low toxicity[13]. Moreover, this strategy can enable the rapid synthesis of highly effective compounds that are already clinically approved, ultimately shortening the drug commercialization pipeline.

Isoniazid (INH), a first-line anti-TB drug, is the most powerful agent used to treat *M. tuberculosis* infection since 1952[14]. It is a pro-drug requiring activation *via* enzyme catalase-peroxidase encoded by *katG* to its active form[15]. The activated metabolite of INH inhibits the synthesis of mycolic acid, a vital component of the mycobacterial cell wall, by targeting the enoyl-ACP reductase InhA of the type II fatty acid synthase[16–18]. The decrease in catalase-peroxidase activity as a result of *katG* mutations is considered as the most common mechanism associated with INH resistance[19]. Among all the genes involved in INH resistance, excluding *katG*, mutations of InhA confer clinically relevant levels of resistance to INH. Multiple other genes such as *nat* coding for *N*-acetyltransferase (NAT) contribute to resistance to INH in *M. tuberculosis* before KatG activation. Furthermore, both NAT and KatG enzymes interact with the pro-drug directly[20]. Following INH metabolism in the liver, hydrazine metabolites (nitrogen-centered free radicals) are produced which generate highly reactive oxygen species and act as a stimulator of lipid peroxidation, resulting in cell death and hepatic necrosis[21,22]. As INH is the major therapeutic arsenal in the treatment of TB infection, continuous efforts are being made to develop new INH derivatives with greater activity, low cytotoxicity, and fewer side effects[23–24]. Several current reports show that the amalgamation of hydrophobic moieties into the basic structure of INH can enhance the penetration of the drug into the lipophilic cell wall of the bacterium[25]. Further, the *N*-acetyltrans-2 (NAT2) promoted inactivation of INH could also be avoided by functionalizing its hydrazine group[26].

Quinoline moiety is present in a variety of natural products and has diverse biological properties. Notably, quinoline appears as a central core in the recently developed anti-TB drugs such as TMC 207 or

* Corresponding author.
E-mail address: vipan_org@yahoo.com (V. Kumar).

https://doi.org/10.1016/j.bmcl.2020.127576
Received 28 July 2020; Received in revised form 19 September 2020; Accepted 21 September 2020
Available online 24 September 2020
0960-894X/

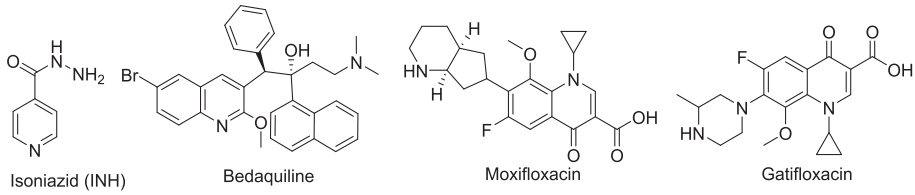

Fig. 1. Chemical structures of standard drug isoniazid (INH) and quinoline based anti-tubercular agents.

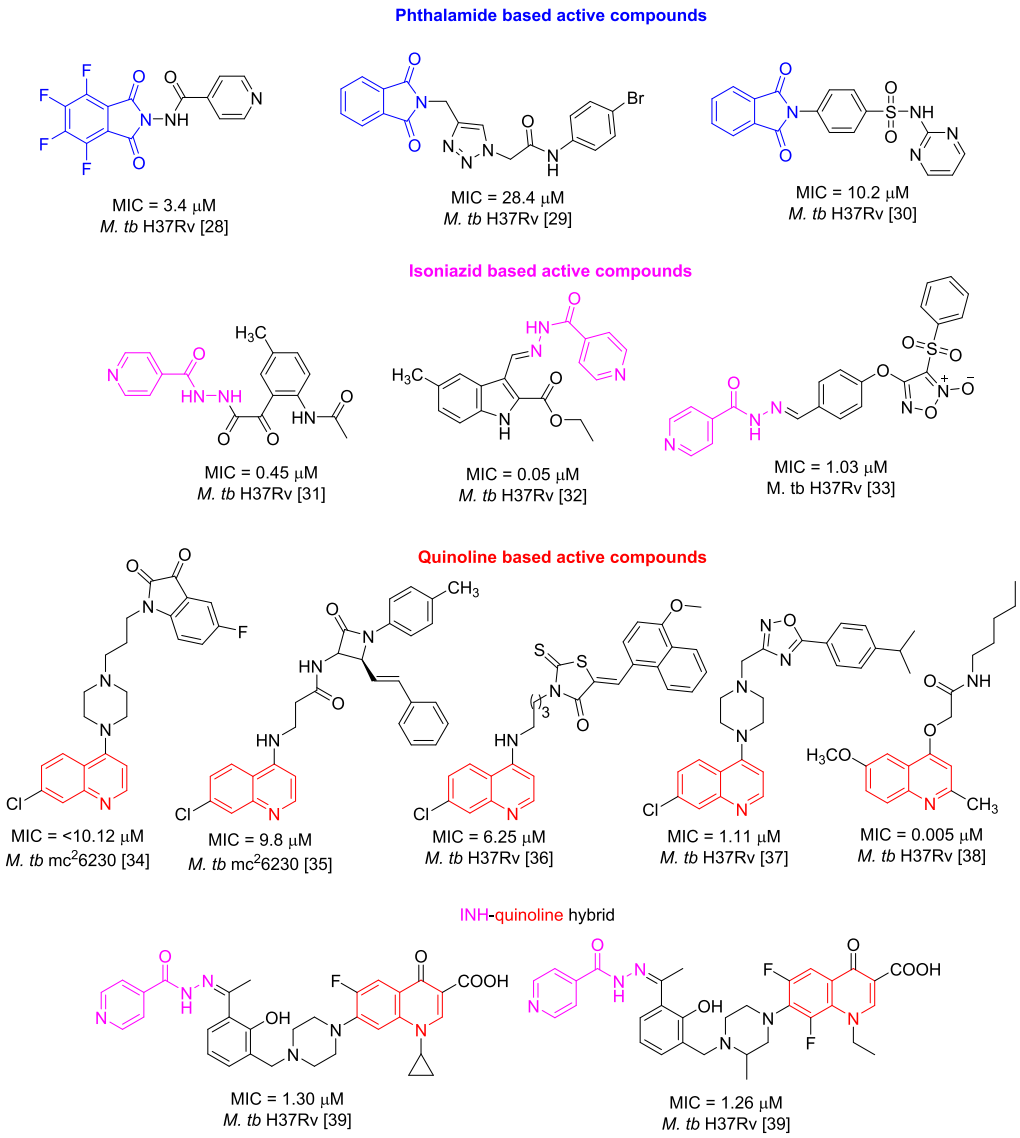

Fig. 2. Promising anti-TB hits with cores highlighted used in the present design.

bedaquiline and some fluoroquinolones *viz.* gatifloxacin, and moxifloxacin (Fig. 1)[27].

Keeping in view the hybrid concept along with the anti-tubercular potential of different moieties (Fig. 2) from the literature [28–39], it was planned to synthesize hybrid compounds that comprise the isoniazid nucleus with the aforementioned fragments and their evaluation of anti-TB activity.

Recently, we introduced a functionalized isoindoline-1,3-diones into the alkyl chain of 4-aminoquinolines to access their anti-mycobacterial potency. The compounds were promising candidates with a MIC of 13.5–14.6 μM against the mc^{2}6230 strain of *M. tuberculosis* (Fig. 3)[40,41]. Motivated by these results and in continuation[42], the present work is a logical extension and involves the synthesis and anti-mycobacterial evaluation of 4-aminoquinoline-isoniazid hybrids linked

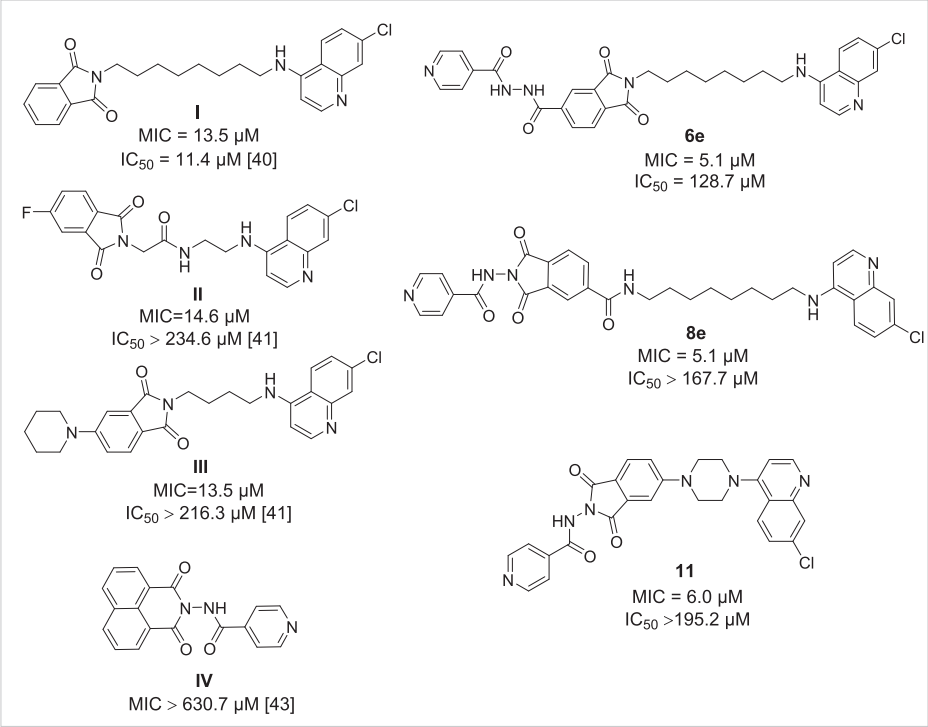

Fig. 3. Comparison of activity against mc^{2}6230 and cytotoxicity against Vero cells of **6e, 8e** and **11** with previously reported scaffolds **I-IV**[40–41,43].

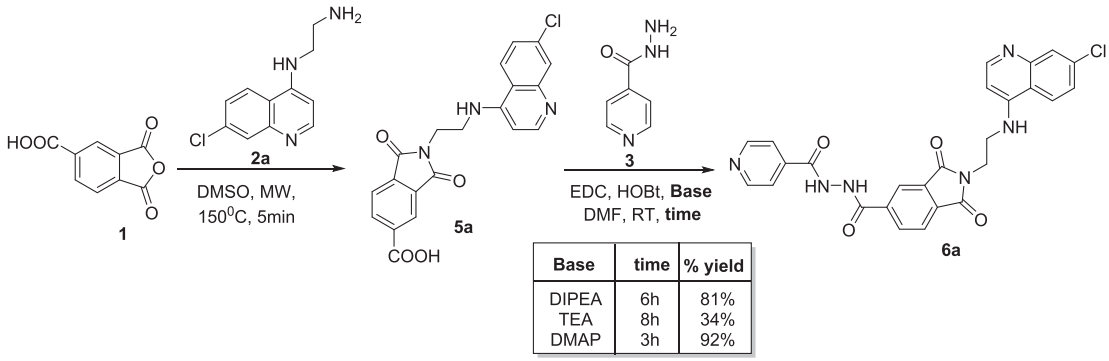

Base	time	% yield
DIPEA	6h	81%
TEA	8h	34%
DMAP	3h	92%

Scheme 1. Optimizing synthesis of the 4-aminoquinoline-isoindoline-dione-isoniazid triad **6a.**

via isoindoline-1,3-diones. The length of the alkyl chain spacer between the pharmacophores along with the position of INH and 4-aminoquinoline around the isoindoline-1,3-dione were meticulously altered to study their influence on Structure-Activity Relationship.

For the synthesis of first series of desired 4-aminoquinoline-isoindoline-dione-isoniazid triads, **6a-e**, the reaction of substituted phthalic anhydride **1** with quinoline based diamines **2** was carried out in DMSO at 150°C for 5 min, in a microwave synthesizer to result in 4-aminoquinoline-isoindoline-diones **5a-e**. EDC-HOBt promoted amide coupling between **5a-e** and isoniazid afforded the corresponding conjugates **6a-e.** Different bases *viz. N, N*-Diisopropylethylamine, triethylamine, 4-Dimethylaminopyridine were screened along with amide coupling reagents in order to optimize the yield (Scheme 1). The best result in terms of yield was obtained with DMAP at low temperature for 3 h.

Another set of 4-aminoquinoline-isoindoline-dione-isoniazid triads,

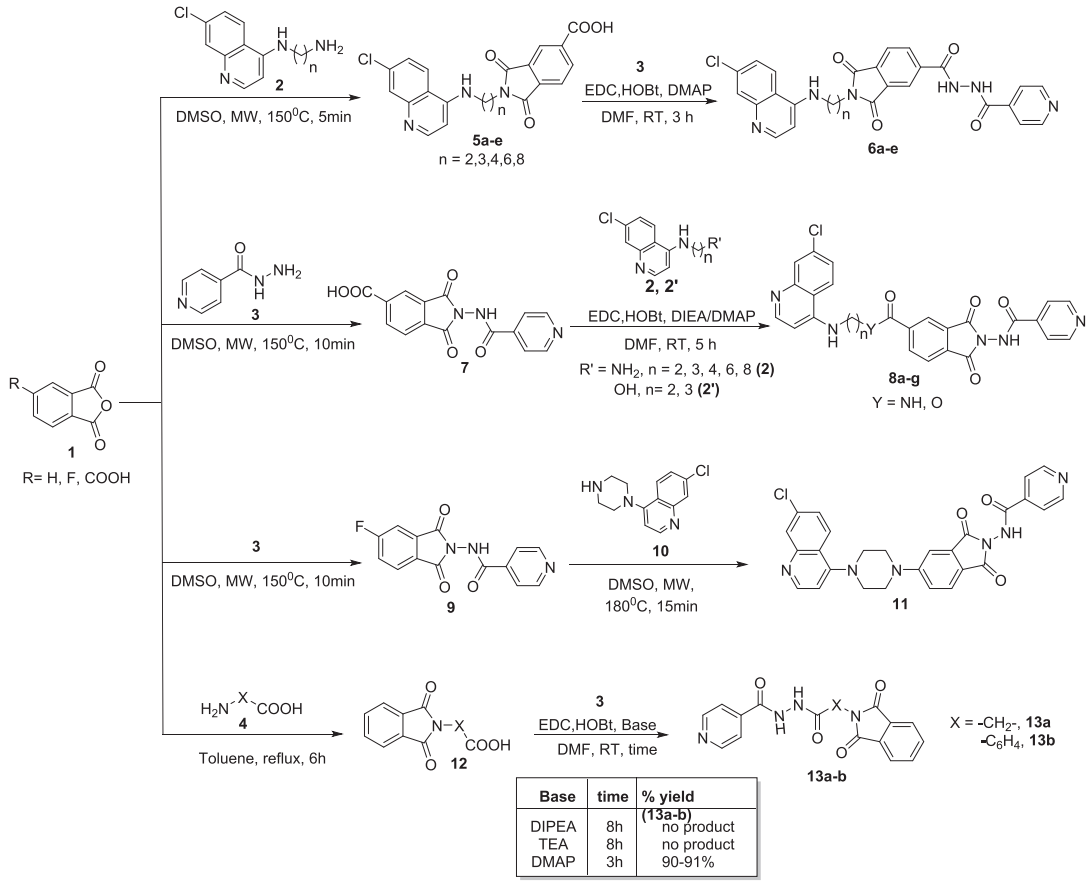

Scheme 2. Synthesis of 4-aminoquinoline-isoindoline-dione-isoniazid conjugates.

8a-g were prepared *via* an initial microwave heating of substituted phthalic anhydride **1** with isoniazid **3** to result in isoniazid-isoindoline-dione **7**. Amide/Ester coupling between **7** and quinoline based diamine **2**/quinoline based alcohol **2′** afforded **8a-g** in good yields. A cycloalkyl *viz.* piperazinyl analogue **11** was also synthesized to determine the influence of alkyl chain on anti-mycobacterial activities. Further, in order to rationalize the anti-mycobacterial effect of quinoline core in the present series of triads, amide-tethered isoniazid-isoindoline-dione conjugates **13a-b** were synthesized *via* an initial treatment of **1** with amino acids **4** to afford **12** with subsequent treatment with isoniazid using standard coupling procedure (Scheme 2). The structures of the synthesized 4-aminoquinoline-isoindoline-isoniazid conjugates were assigned based on the spectral and analytical evidence. For example, the compound **6a** showed a molecular ion peak at 515.1177 in its high-resolution mass spectrum (HRMS). The significant features of its ^{1}H NMR spectrum involved the presence of a triplet at δ 3.82 because of methylene (N-CH_2-); two doublets at 6.62 (J = 5.3 Hz) and 7.76 (J = 2.2 Hz) corresponding to quinoline protons along with a multiplet of isoindoline ring protons at 8.27–8.31. The presence of signals in its ^{13}C NMR spectrum at δ 164.6, 164.7, 167.7, and 167.8 corresponding to imide- and amide carbonyls, along with methylene carbons at 36.5 and 40.7 further validated the assigned structure.

The synthesized 4-aminoquinoline-isoniazid conjugates were assessed for their anti-mycobacterial activities against avirulent *M. tuberculosis* mc^{2}6230 strain and the results are enlisted in Table 1. The cytotoxicity of all derivatives to mammalian Vero cells was also evaluated to establish whether the observed activities were due to their inherent anti-mycobacterial ability or due to cytotoxicity (Table 1). As evident, the compounds showed promising anti-mycobacterial activities, although they were not as active as INH. A closer examination of the results showed the activity dependence on both the length of the alkyl chain between the pharmacophores as well as the position of INH and 4-aminoquinoline around isoindoline core. Among the 4-aminoquinoline-isoindoline-1,3-diones **5a-e** (without INH-core), the compounds lack any anti-mycobacterial activity except **5c** and **5d** with weak activity but cytotoxicity. Inclusion of INH among these conjugates not only improved their anti-mycobacterial activity substantially but also decreased their cytotoxicity as seen in triads, **6a-e**. The improvement in anti-mycobacterial and cytotoxicity profile is apparent at longer chain lengths, as displayed by **6d** and **6e** with MIC_{99} of 21.9 and

Table 1
In vitro anti-mycobacterial activity (MIC_{99}) of synthesized compounds against $mc^2$6230 strain of *M. tuberculosis* and cytotoxicity (IC_{50}) evaluation on mammalian Vero cells and their selectivity index (SI).

Code	Structure	% Yield	MIC_{99} (μM)	IC_{50} (μM)	SI value
5a	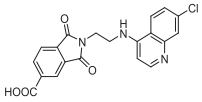	81	> 506.2	> 253.1	> 0.5
5b	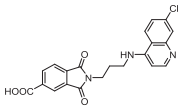	86	488.8	242.0	0.5
5c	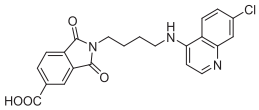	87	236.3	40.1	0.16
5d	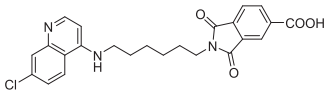	86	221.6	24.3	0.11
5e	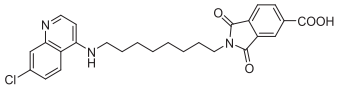	89	417.3	> 208.6	> 0.5
6a	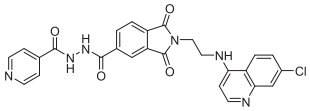	91	389.0	> 194.5	> 0.5
6b	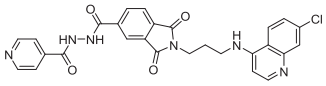	86	47.3	119.2	2.5
6c	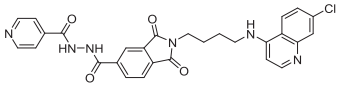	82	23.0	16.6	0.7
6d	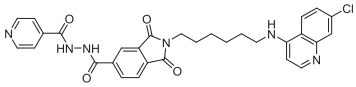	88	21.9	128.0	5.8
6e	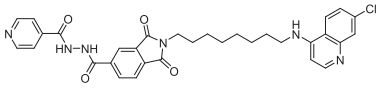	81	5.1	128.7	25
8a	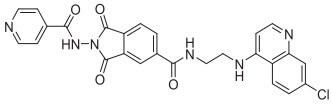	85	6.0	64.1	10.6
8b	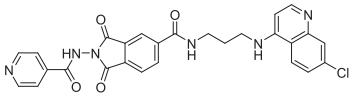	87	5.8	160.9	27
8c	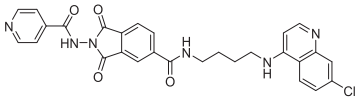	74	23.0	14.7	0.6
8d	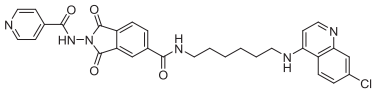	76	11.0	33.3	3
8e	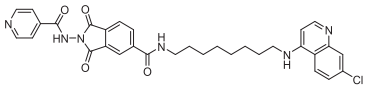	72	5.1	> 167.1	> 32.7
8f	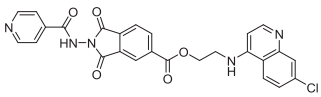	85	> 388.2	> 194.1	> 0.5
8g	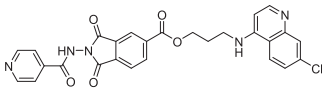	84	11.9	> 194.1	> 16
11	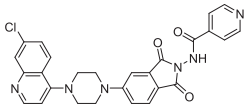	89	6.0	> 195.2	> 32.5

(*continued on next page*)

Table 1 (*continued*)

Code	Structure	% Yield	MIC_{99} (μM)	IC_{50} (μM)	SI value
13a	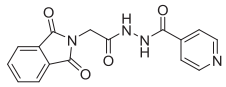	92	308.5	> 308.5	> 1
13b	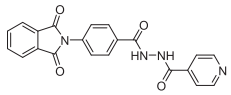	90	129.4	> 258.9	> 2
INH	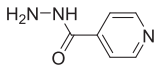	–	0.07		

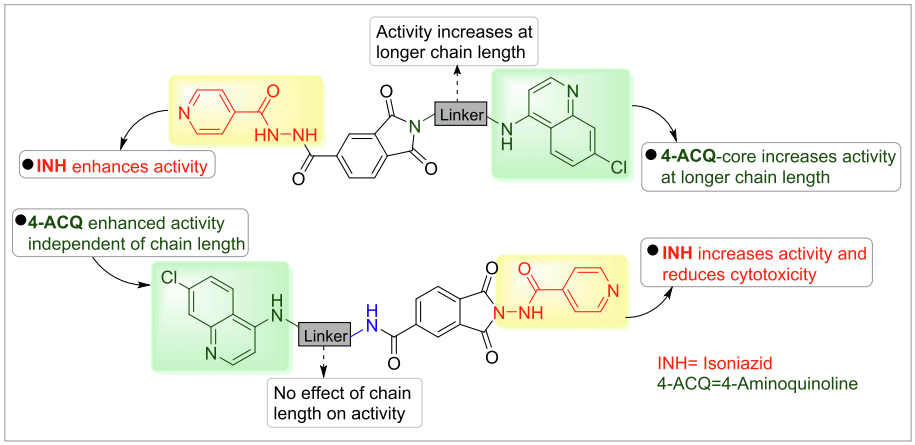

Fig. 4. Structure-Activity Relationship (SAR) of both series of synthesized 4-aminoquinoline-isoindoline-dione-INH triads.

5.1 μM and IC_{50s} of 128 and 128.7 μM, respectively.

Furthermore, interchanging the position of INH with quinoline diamines around isoindoline core in compound **8a-e** improved the anti-mycobacterial activities without much dependence on the alkyl chain length. The triad **8e** with an octyl spacer not only retained the anti-mycobacterial efficacy (MIC_{99} = 5.1 μM), it is also non-cytotoxic ($IC_{50} \geq 167$ μM). The inclusion of a cyclic amine *viz.* piperazine instead of alkyl amine as in triad **11** also resulted in the good anti-mycobacterial activity.

The conjugates, **13a** and **13b** without a quinoline core, did not show any substantial anti-mycobacterial activity; thus, justifying the importance of the proposed design of 4-aminoquinoline-isoindoline-dione-isoniazid triads to elicit anti-mycobacterial activity and reduce cytotoxicity.

Relating the activity and cytotoxicity data of currently synthesized compounds (**6e, 8e, 11**) with our earlier report (**I-IV**)[40–41,43], the introduction of INH at C-5 of isoindoline ring not only improved anti-mycobacterial activity but also resulted in the reduction of cytotoxicity (Fig. 3). The general anti-TB SAR/cytotoxicity of the synthesized series of 4-aminoquinoline-isoindoline-isoniazid triads is elucidated in Fig. 4.

Molecular docking studies and ADME properties prediction

Molecular docking studies were conducted using AutoDock to explore the potential binding interactions of selected compounds with *M. tuberculosis* enoyl-acyl carrier protein reductase (InhA; PDB ID: 4TZK). InhA is a prominent enzyme involved in the biosynthesis of mycolic acid for mycobacterial cell wall and the molecular target of isoniazid. Six inhibitors were docked into the active site of InhA, as shown in Figs. 5 and 6, while the docking results are summarized in Table 2.

In consonant with the experimental results, the binding energies and receptor interactions of compounds **6e**, **8e** and **11** were superior to compounds **I**, **II** and **III** (Table 2). For instance, in compound **I** (Fig. 5**a**), the chlorine atom was sandwiched between residues Phe149 and Met199 *via* hydrophobic interactions while the amino group of quinoline core formed a hydrogen bond interaction with the hydroxyl oxygen of Gly192. The isoindoline core also afforded alkyl, π-π stacking, π-alkyl, and π-σ interactions with Ile95, Phe41, Val65, Ile122, Phe149, and Met199. A similar binding profile was observed for the isoindoline core of compound **II** (Fig. 5**b**), i.e. π-π stacking with residue Phe41 as well as

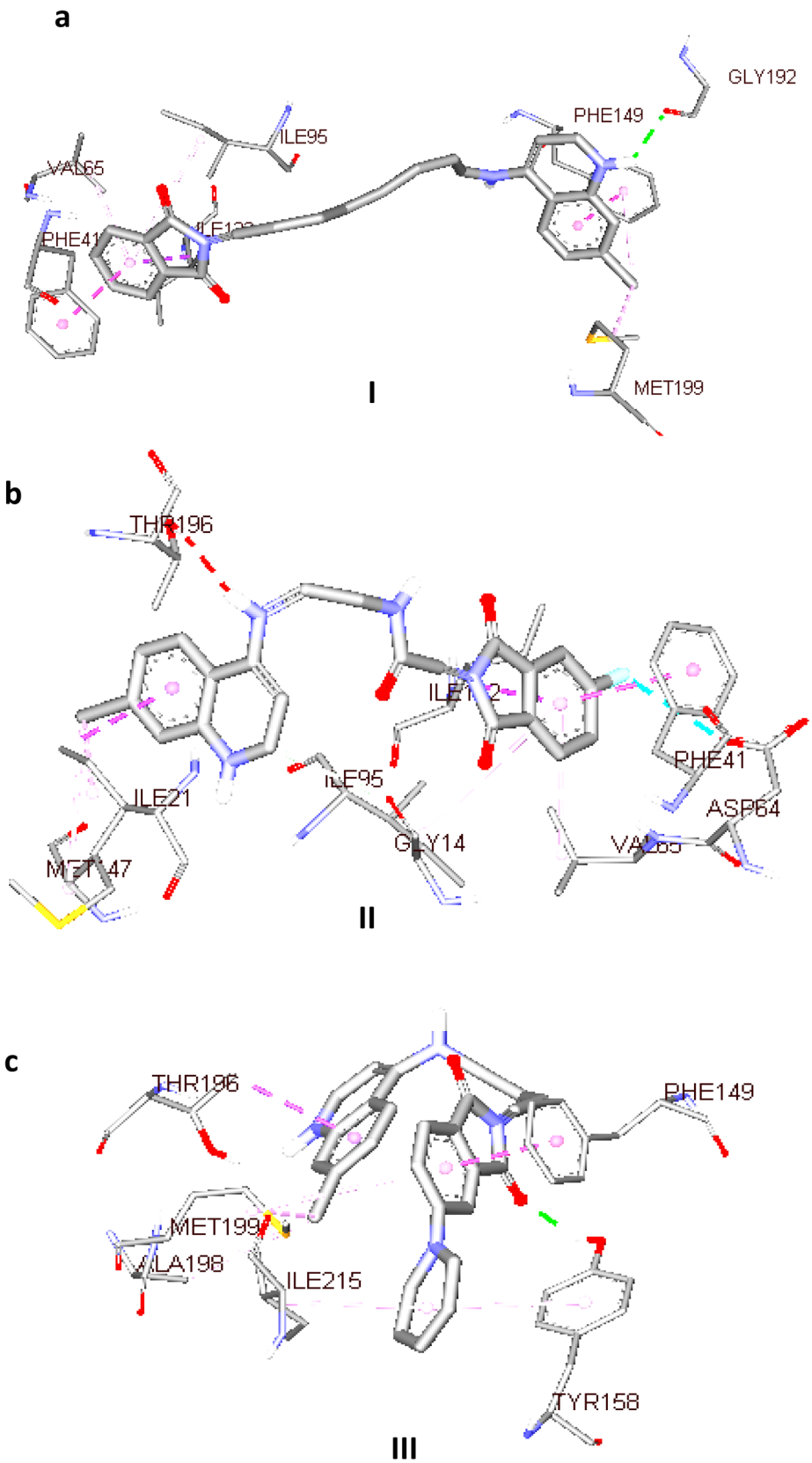

Fig. 5. Binding interactions of compounds (a) **I** (b) **II** (c) **III**.

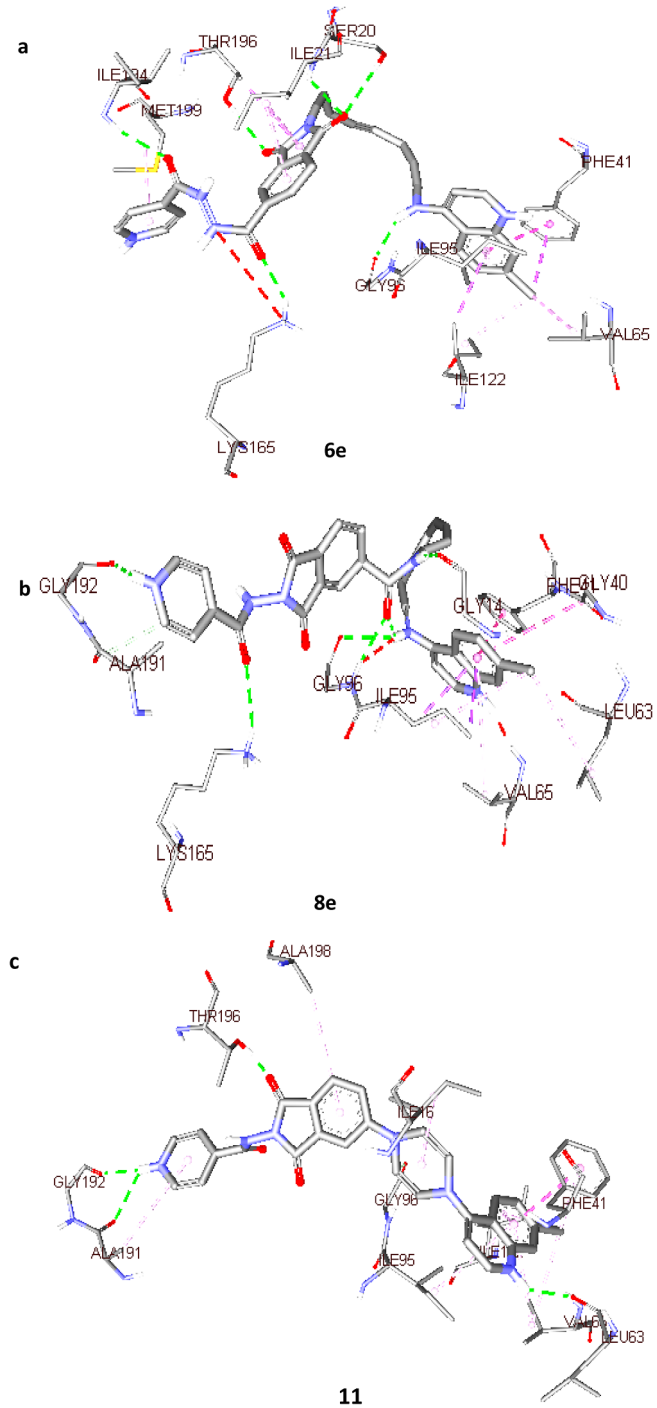

Fig. 6. Binding interactions of compounds (a) **6e** (b) **8e** (c) **11.**

π-σ, π-alkyl, and alkyl interactions with Ile21, Val65, Ile122, Phe149, Ala198, Met147 and Ile95. The unit also featured a hydrogen bond interaction between the isoindoline and Ile95, while the fluorine substituent formed a halogen bond with Asp64. The docked complex of **III** (Fig. 5**c**) was established in the hydrophobic pocket created by hydrophobic interaction with the side chains of ten amino acid residues. Surprisingly, the oxygen atom of the isoindoline core formed a strong hydrogen bond with Tyr168. The interaction was absent in compounds **I** and **II**; hence, a potential platform for further structural modifications to enhance the anti-mycobacterial activity.

Furthermore, compound **6e**, **8e** and **11** binds in essentially the same manner within the active site of InhA. The compound **6e**-InhA complex is characterized by six hydrogen bond interactions between the amino acid residues of side chain and both the oxygen atom of isoniazid moiety and the amine linker. Besides, the quinoline core was anchored in the hydrophobic pocket containing Val65, Ile95, Phe41, and Ile122, which suggested that the two-fold increase in potency might stem from additional interactions between the isoniazid moiety and the side chains of the active site residues (Fig. 6**a**). Furthermore, the isoniazid moiety in compound **8e** interacts with Gly192, Ala191 and Lys165 *via* hydrophobic and H-bonding interactions while the aminoquinoline group formed hydrophobic interactions with residue Val65, Leu63, Gly14 and Gly40, respectively. Other residues that made H-bond interactions include, Gly96, Ile95, Ile165, which also serve as motivators for the stabilization of the inhibitor within the catalytic pocket of the receptor (Fig. 6**b**). Moreover, the docked complex of compound **11** showed additional hydrogen bond interactions between the piperazine ring and the carbonyl oxygen of Gly96, which was accompanied by hydrophobic interaction with Ile16 (Fig. 6**c**).

On the other hand, the molecular descriptors ADME properties were calculated for potent compounds using web-based software pkCSM (http://biosig.unimelb.edu.au/pkcsm/prediction) and SwissADME (http://www.swissadme.ch/). The results are presented in Table 2**.** The drug candidates with TPSA values of 140 Å or lower are expected to have good absorption. Accordingly, all the compounds were within this limit, i.e., < 140 Å, which implies that these compounds fulfilled the optimal requirement for drug absorption.

In conclusion, a series of 4-aminoquinoline-isoindoline-dione-isoniazid triads have been synthesized with the target of reviewing their SAR against *M. tuberculosis*. Nearly all of the synthesized conjugates presented promising anti-TB activity and useful selectivity index. The conjugates without the quinoline core **13a/13b** and the INH nucleus **5a-e** failed to inhibit the growth of *M. tuberculosis* as was observed in our previous report on 1,8-naphthalimide-isoniazid hybrids[43], further validating the design of triads in the present case.

Declaration of Competing Interest

The authors declare that they have no known competing financial interests or personal relationships that could have appeared to influence the work reported in this paper.

Table 2
Molecular descriptors and the binding energy of the potent compounds.

Compound	B.E(kcal/mol)	TPSA	log*P*	HBD	HBA	log*S*	Caco2	log *Kp*	log*BB*
I	−9.7	62.30	5.05	1	3	−5.5	0.465	−2.773	0.133
II	−9.9	91.40	2.77	2	5	−3.716	0.645	−2.816	−1.407
III	−10.2	65.54	4.35	3	3	−4.945	0.76	−2.877	0.231
6e	−10.4	133.39	4.42	3	6	−4.094	0.768	−2.735	−1.745
8e	−10.3	133.39	4.40	3	6	−4.324	1.65	−2.735	−1.544
11	−11.7	98.74	2.27	1	5	−4.044	0.692	−2.767	−1.129

TPSA – Topological Polar Surface Area (60–140); log BB – logarithm of predicted blood/brain barrier partition coefficient (−3.0–1.2); Caco-2 – cell membrane permeability (> 0.9 is high); HBA – number of hydrogen bond acceptors; HBD number of hydrogen bond donors; log K_p – predicted skin permeability(SP) > −2.5 is low.

Acknowledgments

The authors thank the Council of Scientific and Industrial Research, New Delhi, India for funding (AR Ref. No. 09/254(0269)/2017-EMR-I). MDJ received a postdoctoral fellowship from Labex EpiGenMed under the program « Investissements d'avenir » (ANR-10-LABX-12-01). LK acknowledges the support by the Fondation pour la Recherche Médicale (FRM) (DEQ20150331719). PS acknowledges to the National Research Foundation (NRF), South Africa for a Competitive Grant for unrated Researchers (Grant No. 121276), and the Centre for High-Performance Computing (CHPC), Cape Town, for the supercomputing facilities.

Appendix A. Supplementary data

Supplementary data to this article can be found online at https://doi.org/10.1016/j.bmcl.2020.127576.

References

1. (a) World Health Organization, Annual Report, 2017. http://apps.who.int/iris/ bitstream/10665/254762/1/978929022584-eng. pdf (b) K. F. M. Pasqualoto, E. I. Ferreira, O. A. Santos-Filho, A. J. Hopfinger, J. Med. Chem. 47 (2004) 3755. (c) P. Modi, S. Patel, M. Chhabria, Bioorg. Chem. 87 (2019) 240.
2. "Get the Facts about TB Disease" TBFACTS.ORG, http://www.tbfacts.org/ symptomstb.
3. World Health Organization (WHO). Global tuberculosis report. 2019. Available from: https://www.who.int/tb/publications/global_report/tb19_Exec_Sum_12Nov2019.pdf?ua=1.
4. Reddy DS, Kongot M, Netalkar SP, et al. *Eur J Med Chem.* 2018;150:864.
5. Zumla A, Nahid P, Cole ST. *Nat Rev Drug Discov.* 2013;12:388.
6. Cohen T, Becerra MC, Murray MB. *Microb Drug Resist.* 2004;10:280.
7. Chen J, Zhang S, Cui P, Shi W, Zhang W, Zhang Y. *J Antimicrob Chemother.* 2017;72:3272.
8. Deun AV, Maug AK, Bola V, et al. *J Clin Microbiol.* 2013;51:2633.
9. Stanley RE, Blaha G, Grodzicki RL, Strickler MD, Steitz TA. *Nat Struct Mol Biol.* 2010;17:289.
10. Vilcheze C, Jacobs WR. *Microbiol. Spectr.* 2014;2:0014.
11. Lu X, Tang J, Cui S, et al. *Eur J Med Chem.* 2017;125:41.
12. Manosuthi W, Wiboonchutikul S, Sungkanuparph S. *AIDS Res Ther.* 2016;13:22.
13. Anil K, Eric A, Nacer L, Jerome G, Koen A. *Nature.* 2011;469:483.
14. Teixeira VH, Ventura C, Leitão R, et al. *Mol Pharm.* 2015;12:898.
15. Robitzek EH, Selikoff I. *J Am Rev Tuberc.* 1952;65:402.
16. Banerjee A, Dubnau E, Quemard A, et al. *Science.* 1994;263:227.
17. Marrakchi H, Laneelle G, Quemard A. *Microbiology.* 2000;146:289.
18. Vilchèze C, Wang F, Arai M, et al. *Nat Med.* 2006;12:1027–1029.
19. Zhang Y, Heym B, Allen B, Young D, Cole S. *Nature.* 1992;358:591.
20. Nusrath AU, Doss GP, Kumar CT, Swathi S, Lakshmi AR, Hanna LE. *J Global Antimicrobial Resist.* 2017;11:57.
21. Vavríkova E, Polanc S, Kocevar M, et al. *Eur J Med Chem.* 2011;46:4937.
22. Vavríkova E, Polanc S, Kocevar M, et al. *Eur J Med Chem.* 2011;46:5902.
23. Elumalai K, Ali MA, Elumalai M, Eluri K, Srinivasan S. *J Acute Dis.* 2013;2:316.
24. Matei L, Bleotu C, Baciu I, et al. *Bioorg Med Chem.* 2013;21:5355.
25. (a) Sandy J, Mushtaq A, Kawamura A, Sinclair J, Sim E, Noble M. *J Mol Biol.* 2002;318:1071–1083;
    (b) Yuan-Qiang Hu, Zhang S, Zhao F, et al. *Eur J Med Chem.* 2017;133:255.
26. Shingnapurkar D, Dandawate P, Anson CE, et al. *Bioorg Med Chem Lett.* 2012;22:3172.
27. (a) Sundaramurthi JC, Hanna LE, Selvaraju S, et al. *Tuberculosis.* 2016;100:69;
    (b) Villemagne B, Crauste C, Flipo M. *Eur J Med Chem.* 2012;51:1;
    (c) Hoagland DT, Liu J, Lee RB, Lee RE. *Adv Drug Deliv Rev.* 2016;102:55;
    (d) Kumar G, Sathe A, Krishn VS, Sriram D, Jachak SM. *Eur J Med Chem.* 2018;157:1–13;
    (e) Diacon AH, Pym A, Grobusch M, et al. *PLoS ONE.* 2011;6:17556;
    (f) Cohen J. *Science.* 2013;339:130.
28. Elumalai K, Ashraf Ali M, Elumalai M, et al. *Int J Chem Sc.* 2013;4:57.
29. Phatak PS, Bakale RD, Dhumal ST, et al. *Syn. Coumn.* 2019;49:2017.
30. Santos JL, Yamasaki PR, Chin CM, Takashi CH, Pavan FR, Leite CQF. *Bioorg Med Chem.* 2009;17:3795.
31. Branco F SC, Lima EC, de JL, et al. *Eur J Med Chem.* 2018;146:529–540.
32. Velezheva V, Brennan P, Ivanov P, et al. *Bioorg Med Chem Lett.* 2016;26:978.
33. dos GF, Fernandes S, Souza PC, et al. *Eur J Med Chem.* 2016;123:523.
34. Raj R, Biot C, Kremer SC, et al. *Chem Biol Drug Des.* 2014;83:622.
35. Raj R, Biot C, Kremer SC, et al. *Chem Biol Drug Des.* 2014;83:191.
36. Chauhan K, Sharma M, Saxena J, et al. *Eur J Med Chem.* 2013;62:693.
37. Shruthi TG, Eswaran S, Shivarudraiah P, Narayanan S, Subramanian S. *Bioorg Med Chem Lett.* 2019;29:97.
38. Giacobbo BC, Pissinate K, Junior VR, et al. *Eur J Med Chem.* 2017;126:491.
39. Sriram D, Yogeeswari P, Madhu K. *Bioorg Med Chem Lett.* 2005;15:4502.
40. Rani, A. Viljoen, Sumanjit, L. Kremer, V. Kumar, ChemistrySelect, 2 (2017) 10782.
41. Rani A, Viljoen A, Johansen MD, Kremer L, Kumar V. *RSC Adv.* 2019;9:8515.
42. (a) Shalini, A. Viljoen, L. Kremer, V. Kumar, Bioorg. Med. Chem. Lett. 28 (2018) 1309. (b) Shalini, M. D. Johansen, L. Kremer, V. Kumar, Bioorg. Chem. 92 (2019) 103241. (c) A. Singh, A. Viljoen, L. Kremer, V. Kumar, ChemistrySelect 3 (29), 8511.
43. Shalini, M. D. Johansen, L. Kremer, V. Kumar, Chem Bio Drug Design 94, 2019, 1300.